

Wear of hot isostatically pressed (HIPed) thermal spray cermet coatings

V. Stoica, R. Ahmed, Edinburgh/GB, and S. Tobe, Tochigi/J

Verschleißverhalten gehippter TS-Schichten

Das allgemeine Ziel dieser Untersuchungen war es, durch Vergleich von Cermet-Schichten im gespritzten und heißisostatisch gepressten (HIPed) Zustand den gleitenden Verschleiß zu ermitteln. WC-12Co-Schichten wurden mittels HVOF-Spritzern auf ein SUJ-2-haltiges Stahlsubstrat aufgetragen und heißisostatisch mittels Ummantelungstechnik gepresst. Um das gleitende Verschleißverhalten dieser Schichten bei trockener und Schmier-Reibung unter Stahl- und Keramik-Anordnung zu prüfen, wurde eine Hochfrequenz-Austauschvorrichtung (HFRR) verwendet. Die Ergebnisse werden anhand von SEM-Beobachtungen, Verschleißverhalten, Röntgenbeugungs-Befunden, Mikrostrukturuntersuchungen, Mikrohärtebestimmungen und Bruchzähigkeit diskutiert. Erste Ergebnisse deuten darauf hin, dass die HIP-Technik erfolgreich eingesetzt werden kann, um durch Nachbehandlung von thermisch gespritzten Schichten deren Eigenschaften deutlich zu verbessern.

1 Introduction

Over the years, thermal spray coatings proved to be one of the preferred techniques for applying coatings of various materials on substrate which are cheap such as steel. In wear resistant applications, the coated layer provide the resistance to wear whilst the steel support the shock which the system (coating and substrate) is exposed to. Various thermal spraying techniques were employed in order to achieve the best coating properties required for industrial applications. Nowadays, advances in thermal spraying make possible the replacement of bulk components in paper milling [1] or the replacement of chromium plating in aircraft manufacturing [2, 3] or automotive industry [5, 6]. Also the deposition of thermally sprayed coatings on critical parts in petroleum drilling [7], or on components in applications such as fans and high pressure compressors [4, 8] was successful using Detonation Gun spraying (DGun), High Velocity Oxy-Fuel (HVOF) or Atmospheric Plasma Spraying (APS).

To bear the severe wear conditions in life service, a component should have, beside the high hardness, an acceptable level of fracture toughness. It is widely recognized that tungsten carbide-cobalt has the combination of high hardness of tungsten carbide grains with the ductility of metal cobalt. Also, among other carbides, tungsten carbide has the ability to deform plastically without fracturing [9]. These special properties offer an excellent behaviour in applications which require resistance to sliding and abrasive wear.

The parameters of the spraying process and powder particles play an important role in achieving an efficient coating. The balance between thermal and kinetic energy during spraying should control the extensive heating of the powders granules and their velocity. A better understanding of the influence of all factors that are involved in the process of spraying helps in keeping a low temperature of the gas flame whilst increasing the velocity. Thus, an optimum temperature which lower the degree of chemical reactions that occur in powder particles during deposition and high velocity which lower the average dwell time and also promote a mechanical bonding at the formation of coating are needed. HVOF has proved to be one of the best techniques to deposit a wear resistant coat-

ing. HVOF-deposited coatings exhibit less phase transformation and lower porosity compared with other techniques. The high velocity and low temperature experienced by the particles lead to a dense mixture of unmelted, semi-melted particles in a fully melted binder. However, this mixture has the disadvantage of relatively low fracture toughness due to poor bonding at the interfaces between unmelted and semi-melted particles. Also some phase transformations occur and the resulted products which are generally brittle decrease the wear resistance of the coating.

Hot Isostatic Pressing (HIP) as a post treatment of thermal spray coatings has proved its efficiency. Although only a limited number of studies were found in the literature, these investigations have revealed significant improvements in coating properties. The hardness and density of the coating increased while the porosity substantially decreased [10, 11]. It was reported a change from lamellar to granular structure during HIPing [11] and also metallurgical bonding at the splat/splat and coating/substrate interface.

In the present investigation sliding wear resistance of as sprayed and post treated WC-12wt%Co deposited by HVOF was evaluated by reciprocating ball on disk testing. The changes experienced by the cermet coating were explained in terms of microstructure, hardness, fracture toughness and sliding wear resistance.

2 Experimental Procedure

2.1. Coating production and post treatment

The material selected for the evaluation was a sintered WC-Co powder with 12 weight per cent Co. The size distribution measured by optical microscopy ranged from 25-60 μm . The mean particle size value was of 40 μm . **Fig 1** shows the scanning electron micrograph of the powder.

The coatings were produced by HVOF process on discs with diameter of 31mm and thickness of 8mm. Oxygen and hydrogen were mixed in the combustion chamber forming gases that accelerated the powder particles through the nozzle onto SUJ-2 bearing steel substrate. The substrate was grit blasted prior deposition.

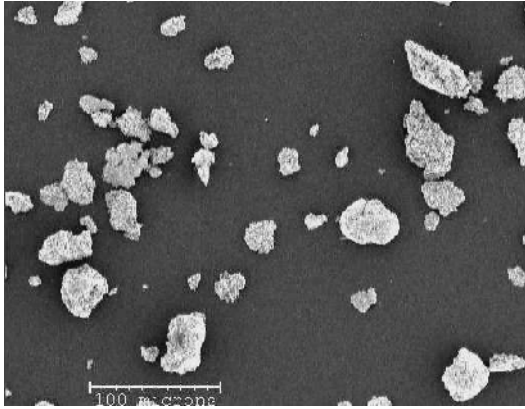


Fig 1. Sintered WC-12Co powder (scale bar: 100 microns)

The HIP treatment was carried out at a fixed temperature and pressure of 850°C and 150MPa, respectively. The samples were encapsulated and heated at a rate of 50°C/h until the desired temperature was reached, after which, they were cooled at a rate of 30°C/h. Then, the pressure was released.

Table 1. HIPing parameters

HIPing parameters	
Temperature	850°C
Pressure	150MPa
Heating rate	50°C/h
Cooling rate	30°C/h

2.2. Coating characterisation

The X-ray diffraction (XRD) analysis was used to quantify the microstructural modification of both the as-sprayed and HIPed coatings. The diffraction patterns were obtained with a D500 diffractometer operating at 40kV and 20mA. CuK α radiation was used and the samples were run at 2 θ from 10° to 90° with a step size of 0.02° (2 θ) and a time of 2s/step.

Coating microstructures were evaluated by Scanning Electron Microscopy using classical imaging with secondary and backscattered electrons (SE and BSE). Microhardness evaluation was performed on the metallographic prepared samples on the surface and on the cross section. Each value presented is an average of thirty-six measurements performed at a load of 300g using a Vickers Microhardness. Care was taken to avoid the edge effect and also the influence of work hardened zone of affecting a neighbouring one. For the cross-section measurements, the samples were mounted in epoxy and indentations were applied at three different depths in the coating. Fracture toughness was measured on the surface using a 15kg macro hardness apparatus. The value which is presented is an average of 10 measurements.

The worn surfaces were studied using scanning electron microscope. The depth of the wear scar was measured by means of profilometry using an interferometer.

2.3. Tribological testing

Sliding wear tests were carried out using a reciprocating ball-on-plate apparatus instrumented to measure the frictional force via a load cell. Balls fabricated from 440C steel and silicon nitride ceramic were used in this study. The specimens were grounded and polished to produce a near-mirror surface. Before each test, the as-sprayed and HIPed samples and also the balls were ultrasonically cleaned in acetone for 5 minutes to remove any contaminants or grease, dried in air and weighted. The conditions employed in the tests are: load 6kg, sliding speed 0.012m/s at the center of the sample and atmospheric conditions. The difference in weight was used to calculate the volume loss of material during each test and therefore the wear coefficient of each couple in contact.

3. Experimental Results

3.1. Microstructural identification

3.1.1 X-ray diffraction

Fig. 2, a) and **b)**, shows the XRD diffraction patterns for the sintered powder and as-sprayed coating. **Fig. 2c)** shows the results for HIPed coating.

The powder spectrum shows only tungsten carbide (WC) and cobalt (Co) peaks. Small amount of secondary phase are also present probably produced during the sintering process of powder manufacture. X-ray spectra of as-sprayed coating indicate the occurrence of higher amounts of secondary phase of tungsten carbide (W₂C) than in the powder and some eta phases Co₃W₃C. This was expected since all published literature describing HVOF deposited coatings confirm that some degree of phase transformations cannot be avoid during the deposition. Thus no metallic Co was observed in the coating after deposition suggesting that part of metallic tungsten and carbon resulted after decomposition reactions diffused in cobalt. Therefore, an amorphous or nanocrystalline binder phase was produced. This is consistent with other investigations where the same peak broadening that indicates an amorphous or nanocrystalline phase was present in the spectra at 2 θ of approximate 42°. The tungsten that did not dissolved in the matrix is seen in the as-sprayed coating. After post treatment at 850°C in argon environment, all the secondary phase W₂C was eliminated from the coating. Mono tungsten carbide was not affected and higher peaks of eta phases than in the as-sprayed coating were seen. The Co₃W₃C transformed to Co₆W₆C whilst new peaks of Co₃W₃C occurred. The amorphous or nanocrystalline phases can not be seen in the HIPed coatings. Nerz [12] indicated the recrystallisation of the cobalt from the amorphous phase occurred at around 860°C. The recrystallisation reaction led to the occurrence of a large amount of cobalt-containing phases (Co₃W₃C and Co₆W₆C) and, as mentioned before, to the elimination of the broad maxima at 2 θ of approximate 42°.

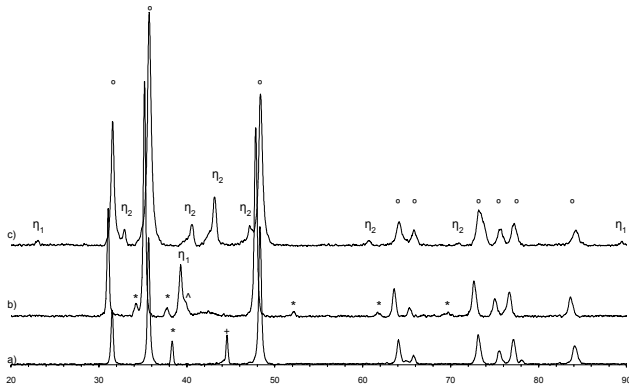


Fig. 2. XRD spectra for a) powder, b) as-sprayed HVOF coating and c) HIPed coating. “ ω ” - WC, “*” - W_2C , “ Λ ” - W, “+” - Co, “ η_1 ” - Co_3W_3C , “ η_2 ” - Co_6W_6C

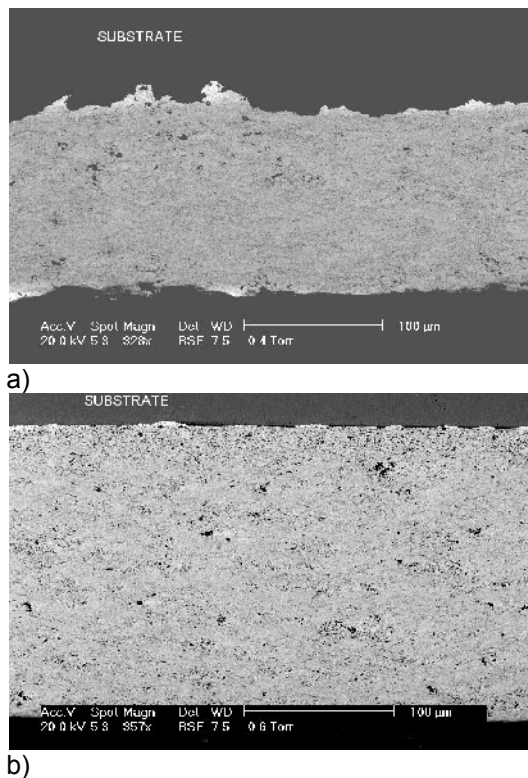


Fig. 3. SEM micrographs on cross-section of as a) as-sprayed and b) HIPed coatings

3.1.2 SEM observations

In addition to phase transformation investigation, the microstructure of both as-sprayed and HIPed coatings was evaluated using the scanning electron microscope. Preliminary results of electron-scanned cross-sections of the as-sprayed and HIPed coatings are shown in **Fig. 3, a) and b)**.

The porosity of all coatings could not be measured at this time. However it is believed that, if the as-sprayed coatings had a certain level of porosity, the densification followed by the HIPing process produced coatings with virtually zero porosity. It is also believed that the dark spots which can be seen on the micrographs

originate from the grinding and polishing (particle pull-out).

It is worth noting the changes that occur on the interface between the coating and the substrate. The roughness of the substrate can be seen clearly in **Fig. 3a)**, thus mechanical interlocking being achieved between the coating and the substrate. Under the pressure and temperature of HIPing process the steel substrate is pressed until the asperities which form the roughness of the steel surface are plastically deformed. Therefore a smooth interface is observed. Any diffusion of steel in the coating material is however the subset of ongoing investigation. Micrographs of cross sections at higher magnification are hence not included here. However, a close examination of these micrographs revealed a phenomenon that occurred preferentially near the substrate/coating interface. This is the precipitation of needle-shaped WC grains at high temperatures of HIPing process.

Comparison between higher magnification of as-sprayed and post-treated coating cross-section micrographs reveals difference in tungsten carbide grain size morphology. The as-sprayed coating has grains which are slightly larger than that of HIPed coating. Beside the fact that the grains are finer, they seem to be more interconnected in the HIPed coating.

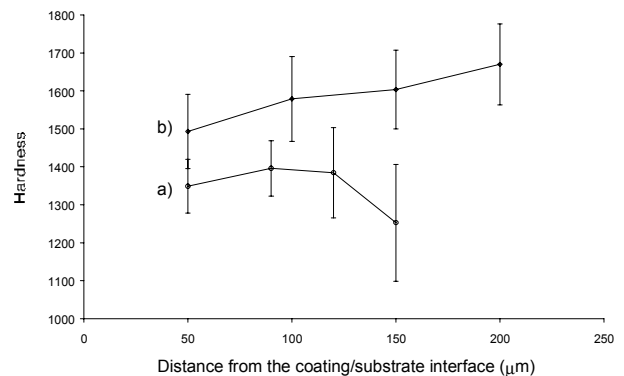


Fig. 4. Variation of microhardness with the distance from the coating/substrate interface. a) as-sprayed coating; b) HIPed coating

3.2. Mechanical testing

The microhardness values for both as-sprayed and HIPed coatings and also the fracture toughness are listed in **Table 2**. The microhardness was measured on the surface and on the cross section at three different depths in the coating. Variation of the hardness with the distance from the interface between the coating and the steel substrate is shown in **Fig. 4**.

An increase in microhardness of the coating after HIPing post treatment which ranges from ~10% at 50μm from the interface to ~30% at the surface of the coatings was observed in this analysis. This increase is related to the phase transformations that occurred during post-treatment of the coating. The hardening of the amorphous phases through recrystallisation reactions led to an overall increase in the hardness of the coating.

Also, the microstructure of HIPed coating with smaller sized and interconnected carbide grains may be a reason for higher hardness. The general behaviour is that microhardness increases with the distance from the interface though the as-sprayed coating shows a slight decrease as the surface was reached.

Table 2. Microhardness and fracture toughness

	HV		K _c [MPa m ^{1/2}]
	As-sprayed	HIPed	As-sprayed
50µm	1348.8	1493	-
100µm	1395.9*	1578.8	-
150µm	1384.4*	1603.5	-
Surface	1252.7	1670	5.2

*The values were measured at 90 and 120µm, respectively because of the limited thickness

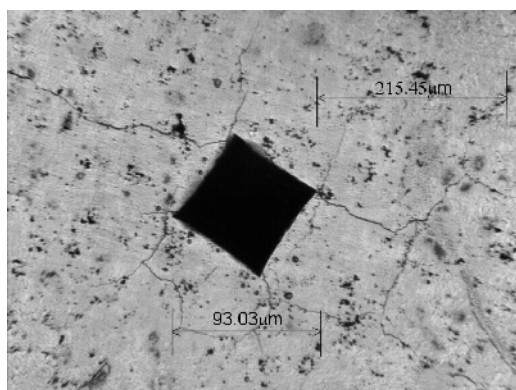


Fig 5. Optical micrograph of fracture toughness indentation (as-sprayed coating) - 15kg load

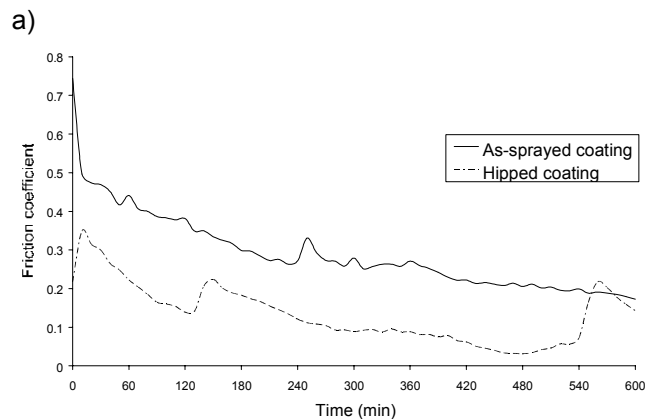
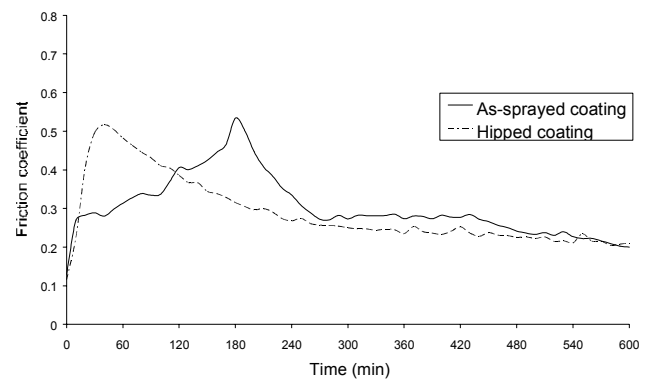
The indentation fracture toughness was measured and calculated according to [14]: $K_c = 0.025 \cdot E^{1/2} \cdot a \cdot P^{1/2} \cdot C^{-3/2}$, where E is the coating Young's modulus (assumed to be 300GPa), P the applied load, 2a the diagonal of the diamond indentation and C the crack length. For the as-sprayed coatings the cracks were seen even at a load of 5kg. However the crack length criterion $C > 2a$ was not reached at this load. Thus, the load was increased, the value presented being measured and calculated at a load of 15kg. At the same load applied on the HIPed coating it could not be observed any cracks. This suggested that beside an increase in hardness the HIPing post treatment led also to an enhancement of the ductility of the coatings.

3.3. Tribological testing

3.3.1 Friction behaviour

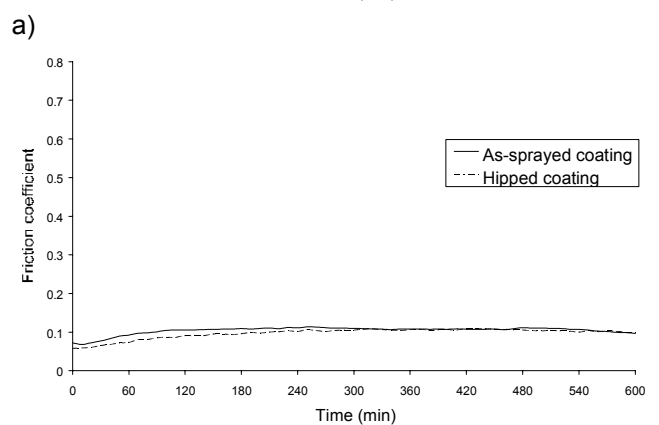
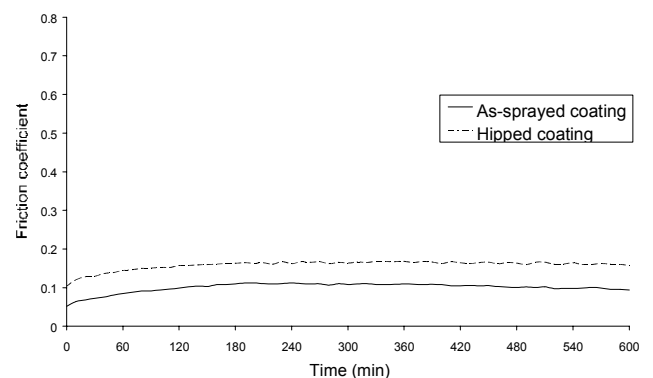
The friction behaviour of all tested configurations (couples) is shown in **Figs. 6** and **7**.

For all tested couples, both in lubricated and dry tests, friction coefficient increased when the ball, steel or silicon nitride (Si_3N_4) is sliding against post treated



b)

Fig.6. Friction coefficients for as- sprayed and HIPed coatings in dry contact against a) SUJ-2 steel and b) Si_3N_4



b)

Fig. 7. Friction coefficients for as-sprayed and HIPed coatings in lubricated contact against a) SUJ-2 steel and b) Si_3N_4

coatings with only one exception. This general behaviour can be related to the improvement achieved in the hard-ness and density of the coatings after the post treatment. When sliding steel balls on coatings in dry contact the friction coefficient shows a running-in stage followed by a decrease and a stabilisation at a value of about 0.2 at the end of the tests. When the as-sprayed coatings are used, the friction coefficient increases in 2 hours from around 0.12 to a maximum of around 0.53. After this stage, the friction coefficient decreases until it reaches the constant value mentioned above after 10 hours. In the case of hipped coating, the end of the first stage is reached only after approximately 1/2 hour. Against the ceramic, the as-sprayed coating doesn't exhibit the running-in stage, the friction decreasing from the maximum value obtained, ~ 0.75 , to a value of 0.2 after 10 hours. The friction coefficient fluctuates, behaviour that can be related to the amount of debris generated during the wear process. Therefore, although the behaviour of the friction during the tests is different depending on the couple, at the end of the tests, same value of the friction coefficients of about 0.2 was noted. As expected, much lower friction coefficient are produced in lubricated tests. The friction coefficient value was not altered after post treatment. In fact, it was surprising to note that the friction of the hipped coating was slightly higher than that of the as-sprayed coating.

The lubricated contact which involved ceramic ball revealed the same friction coefficients for both the as-sprayed and hipped coatings. The friction increased from an initial value which depends on the tested couple to a maximum value which remained approximately constant for the rest of the test. The treated coatings performed better in contact with both steel and ceramic balls than the as-sprayed coatings, the difference being approximately 0.02.

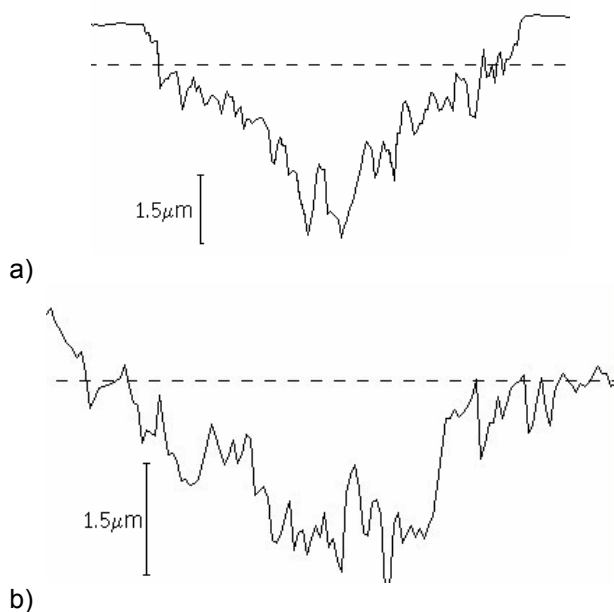


Fig. 8. Wear scars of dry contact for a) as-sprayed coatings and b) hipped coatings vs SUJ-2 steel

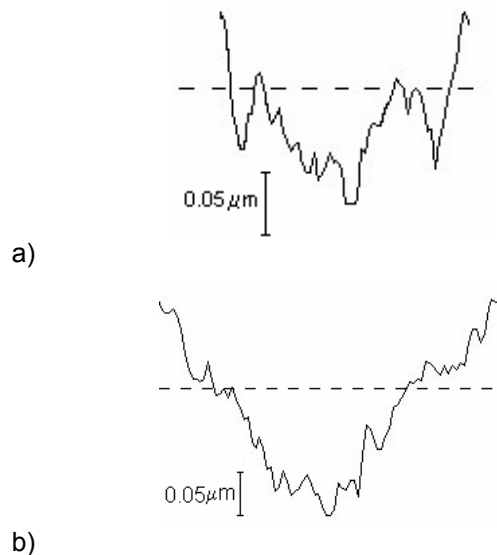


Fig. 9. Wear scars for a) as-sprayed and b) hipped coatings against Si_3N_4 in lubricated tests

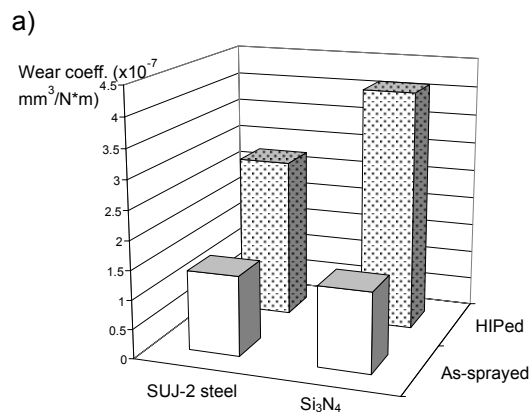
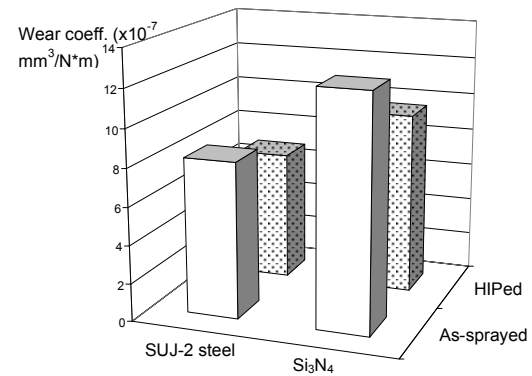


Fig. 10. Wear coefficients a) dry tests; b) lubricated tests

3.3.2 Sliding wear

Fig. 8 exhibits the wear scars of the tests performed in unlubricated condition with the steel ball. These dry tests are characterised by a wide wear scar with a width of $\sim 1.2\text{mm}$ and a depth of $\sim 3.5\mu\text{m}$. Although the wear scars produced by the ceramic ball are not included here, less deep scars were observed with a

depth of about $2\mu\text{m}$. The former scars were much rougher, the asperities suggesting that abrasion produced by the debris is the main wear mechanism. In the later case, the wear scar is wider and featureless. This may be related to the higher hardness of the silicon nitride ball. Compared with these profiles, the wear scars resulting from the lubricated tests are much shallower. The depths of these wear scars are approximately $0.3\mu\text{m}$ when using ceramic ball and $1.5\mu\text{m}$ when using steel ball. All the post-treated coatings which worn in dry contact, exhibit a scar area lesser deep and wide than the as-sprayed coatings. Conversely, the lubricated tests produced deeper and slightly wider wear scar for the hipped coatings than for the as-sprayed ones (**Fig.9**).

Correspondingly, the wear coefficients of the hipped coatings which worn in oil, as depicted from **Fig. 10b**, are greater than those which were not post treated. A reason could be the level of porosity which if any, it is higher in the as-sprayed coatings than in the hipped coatings which in lubricated tests can be beneficial in terms of volume loss of material.

However, this hypothesis was not confirmed by the measurements of porosity in both types of coatings and further investigations have to be carried out.

The values of wear coefficient for unlubricated tests – **Fig. 10a** – demonstrate that the coating post treatment led to a better sliding wear resistance when both steel and ceramic balls were used.

4. Discussion

The wear rates of all couples with some exceptions shows that the sliding wear resistance of the post-treated coatings is higher than that of the as-sprayed coatings. This is related to the modifications that take place in the coating microstructure and also in the phase composition during the process of HIPing. It was seen that even with the best thermal spray process, the deposition of coatings produces a certain degree of chemical reactions leading to secondary phases and also amorphous phases.

The published literature on the post-treatment of thermal spray coatings confirms that the recrystallisation temperature of these amorphous phases is around 860°C [12, 13]. At the HIPing temperature of 850°C employed in this investigation, the recrystallisation reactions took place producing significant changes to the phase composition of the as-sprayed coatings. The elimination of the secondary phase W_2C promotes a higher resistance to wear because, beside the fact that it is harder than WC, it has the disadvantage of being brittle, therefore decreasing the fracture toughness. Although a quantitative evaluation of the fracture toughness of post treated coatings could not be carried out due to the absence of cracks at the applied load, it is clear that this was due to the elimination of brittle phases during the treatment. Moreover, the results of hardness measurements shows a clear increase in the hardness of the hipped coatings. The formation of new carbide phases which replace the amorphous phases from the as-sprayed coatings pro-

duced coatings that are harder than the untreated ones. In addition, the WC grains of the treated coatings were found to be slightly finer and more uniform distributed which helped the formation of harder coatings.

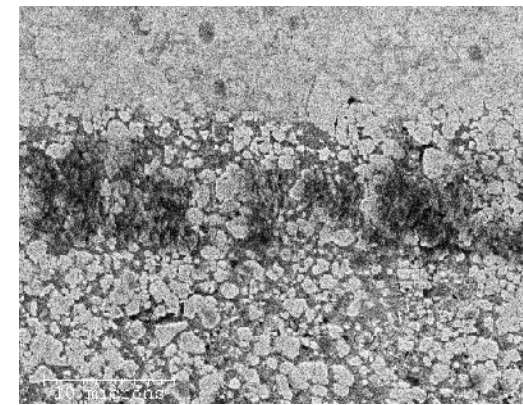
Therefore, both the improved hardness and fracture toughness of the coatings are the main properties that led to a higher wear resistance.

4.1. Wear Mechanisms

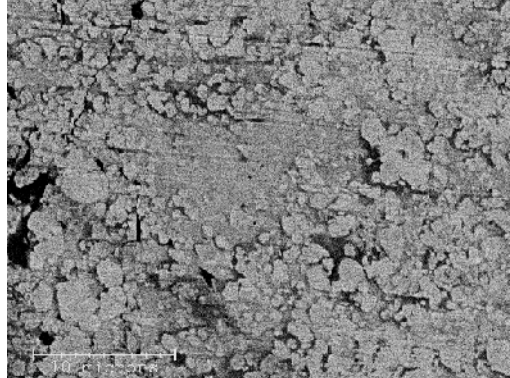
The SEM micrographs shown in **Fig. 11a**) of the as-sprayed which was tested against the steel ball exhibits, at higher magnification, traces of plastic deformation along the entire length of the wear scar. The matrix was seen to be removed by the harder ball (steel) leaving the carbide grains protruding from the matrix. Small traces of abrasive wear were also observed on both matrix and carbide surfaces suggesting that the steel material was also removed by the protruded carbide acting as a three-body abrasive. Contrary to this, the micrographs of the hipped coating tested in the same conditions, **Fig. 11b**), do not exhibit any plastic deformation. As in the as-sprayed coating, the matrix was abraded by the ball steel leading to material removal. Although an analysis of the debris could not be carried out at this stage, it is believed that the debris formed preferentially from the matrix material and the steel ball. Any abrasive marks on the carbide grains were not observed.

The as-sprayed coating tested against ceramic counterpart exhibited abrasive wear as the main wear mechanism, **Fig. 12a**). On this coating, the abrasive marks covered both the matrix and WC grains. The debris might contain beside the steel material, fine particles of WC grains which generate more wear, acting as three-body abrasion. Also, cracks perpendicular on the ball direction was seen in the micrograph. This implies that the binder material could not bear the load applied, the cracks developing along the matrix, at the boundary between carbide grains. The hipped sample, **Fig. 12a**), has almost the same appearance as that hipped sample which slid against the steel ball. Although no cracks were seen in the fracture toughness tests, higher magnification micrographs revealed smaller cracks which were, as in the as-sprayed coating, perpendicular on the sliding direction. It could not be observed any spallation or delamination of the coating material.

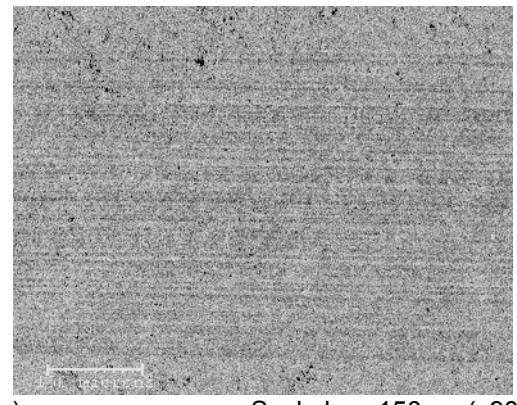
Figs. 11c) and **12c**) show the scanning electron micrograph of the as-sprayed and hipped coatings tested against steel ball in Vitrea-68 oil. Although the two wear scars show almost same characteristics, the abrasive marks of the as-sprayed coating seem to be more pronounced than those existent on the hipped coating. Thus, the micrographs suggest that the abrasive wear is the main wear mechanism that occurs during the lubricated tests. Testing the coatings against Si_3N_4 balls confirm that lubrication mitigate the friction between the mate materials producing wear scars less wide and deep than the dry tests, wear scars that exhibit only low level of abrasive marks.



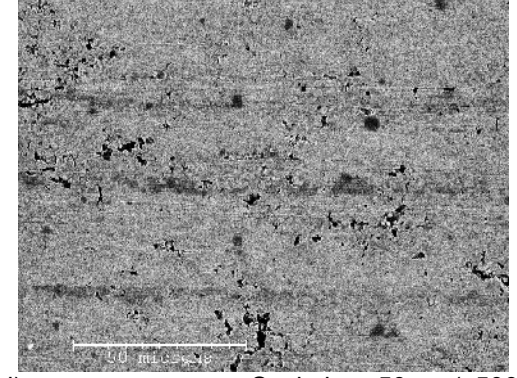
a) Scale bar: 10µm (x1800)



b) Scale bar: 10µm (x2000)

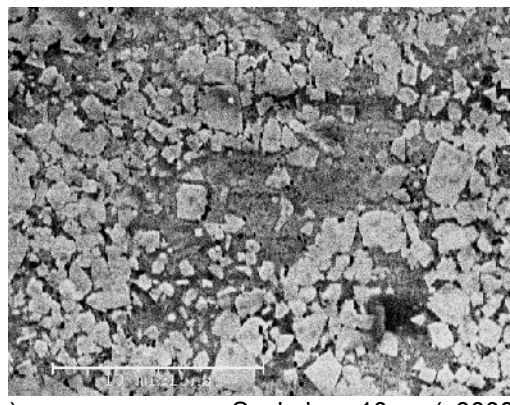


c) Scale bar: 150µm (x90)

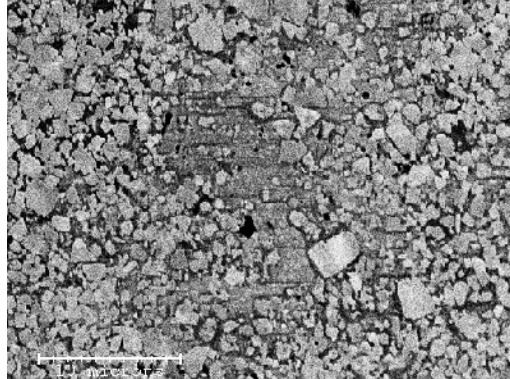


d) Scale bar: 50µm (x500)

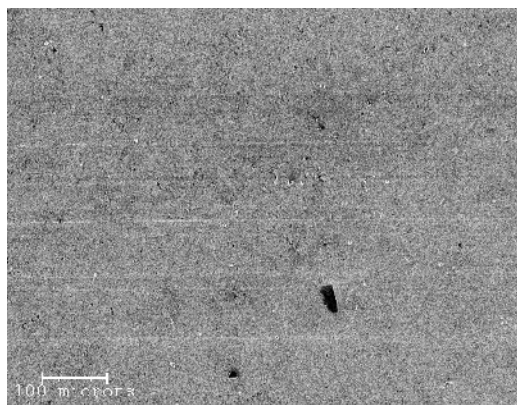
Fig 11. Scanning electron micrographs of the wear scar of as-sprayed coatings in dry and lubricated contact with a), c) SUJ-2 steel and b), d) Si_3N_4



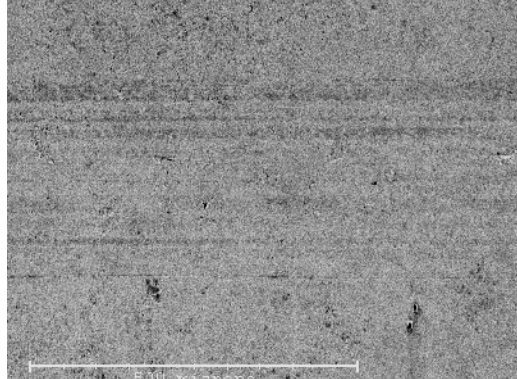
a) Scale bar: 10µm (x3000)



b) Scale bar: 10µm (x2000)



c) Scale bar: 100µm (x90)



d) Scale bar: 500µm (x500)

Fig 12. Scanning electron micrographs of the wear scar of hipped coatings in dry and lubricated contact with a), c) SUJ-2 steel and b), d) Si_3N_4

5. Conclusion

Hot Isostatic Pressure as a post treatment of thermal spray coatings was seen to improve the microstructure, physical properties and, correspondingly, the wear resistance of the coatings. The precipitation of the eta carbides, the elimination of secondary phase W_2C , the changes that occurred in the microstructure due to densification of the coating followed by the HIPing treatment produced harder and tougher coatings. These two properties were seen to promote the achievement of wear resistant coatings. The wear mechanisms in dry tests were the extrusion of matrix material followed by the mechanism of three-body abrasive wear. Also the fracture in the matrix surface was observed. The effect of these mechanisms on the as-sprayed coatings was higher than in the HIPed coatings. The lubricated tests revealed only traces of abrasive wear which were less pronounced than the abrasive marks found on the coatings after dry tests.

References

- [1] A. Fritsch, R. Gradow, A. Killinger, p. 1051-1055
- [2] E. Strock, P. Ruggiero, D. Reynolds, Thermal Spray 2001: New Surfaces for new millennium, Ed. C.C. Berndt, K.A. Khor and E.F. Lugscheider, p. 671-676
- [3] M.N. Nascimento, R.C. Souza, I.M. Miguel, W.L. Pigatin, H.J.C. Voorwald, Surf. Coat. Technol. 138 (2001), p. 113-124
- [4] J.A. Peters, F. Ghasripor, Proc. of the 8th Nat. Spray Conf., 11-15 Sept. 1995, Houston, Texas, p. 387-392
- [5] J. Khedkar, A.S. Khanna, K.M. Gupta, Wear 205 (1997), p. 220-227
- [6] A. Chandak, R. Sivakumar, G. Balasubramanian, p. 531-53
- [7] M.K. Keshavan, K.T. Kembalyan, Proc. of the 1993 Nat. Spray Conf., Anaheim, CA, 7-11 June 1993, p. 635-641
- [8] PM Special Feature, March 1998, p. 26-33
- [9] K. Jia, T.E. Fisher, B. Gallois, NanoStruct. Mat. 10 (1998), p. 875-891
- [10] H. Ito, R. Nakamura, Therm. Spray Research and Applic., Proc. of the 3rd Nat. Therm. Spray Conf. (1990), p. 233-238
- [11] H. Kuribayashi, K. Suganuma, Y. Miyamoto, M. Koizumi, Am. Ceram. Soc. Bull. 65 (1986), p. 1306-1310
- [12] J. Nerz, B. Kushner, A. Rotolico, J. Therm. Spray Technol. 1 (1992), p. 147-152
- [13] C.-J. Li, A. Ohmori, Y. Harada, J. Mat. Sci. 36 (1996), p. 785-794
- [14] P. Ostojic, R. McPherson, Mat. Forum 4 (1987), p. 247-255